Chemical Physics Letters 580 (2013) 130–134

Contents lists available at SciVerse ScienceDirect

Chemical Physics Letters

journal homepage: www.elsevier.com/locate/cplett

Fluorescence quantum efficiency of CdSe/CdS magic-sized quantum dots functionalized with carboxyl or hydroxyl groups

Viviane Pilla [a,*], Sthanley R. de Lima [a], Acácio A. Andrade [a], Anielle C.A. Silva [b], Noelio O. Dantas [b]

[a] Grupo de Propriedades Ópticas e Térmicas de Materiais (GPOTM), Instituto de Física, Universidade Federal de Uberlândia-UFU, Av. João Naves de Ávila 2121, Uberlândia, MG 38400-902, Brazil
[b] Laboratório de Novos Materiais Isolantes e Semicondutores (LNMIS), Instituto de Física, Universidade Federal de Uberlândia-UFU, Av. João Naves de Ávila 2121, Uberlândia, MG 38400-902, Brazil

ARTICLE INFO

Article history:
Received 5 June 2013
In final form 2 July 2013
Available online 8 July 2013

ABSTRACT

The present letter reports the thermo-optical properties of functionalized CdSe/CdS magic-sized quantum dots (MSQDs) (sizes 1.9–2.3 nm) with carboxyl (R–COOH) or hydroxyl (R–OH) groups in aqueous solutions. Atomic force microscopy and infrared transmittance measurements were used to determine the size of the QDs and to highlight the functionalized groups. Absolute nonradiative quantum efficiency (φ) and radiative quantum efficiency (η) values were determined by applying two techniques: thermal lens (TL) and an alternative method that analyzes the ring patterns generated in a laser beam due to thermally induced self-phase-modulation effects known as the conical diffraction. Fluorescence measurements corroborate the TL results.

1. Introduction

Nanostructured semiconductors, or quantum dots (QDs), and bio-conjugated QDs are developing materials that hold potential for a variety of new applications, including uses as efficient biodiagnostic probes for the treatment of diseases, bioimaging, biosensors, biomarkers, drug delivery and engineered tissues [1–4]. Surface passivation and functionalization of QDs are important methods that can improve their nanomaterial properties [5]. Recently, a new class of CdSe QDs known as magic-sized quantum dots (MSQDs), with have sizes from 1 to 2 nm and well-defined structures, has attracted considerable attention because of the dots' novel physical properties [6,7]. The most attractive features are high stability during and after growth [8], closed-shell structures [6], strong quantum confinement similar to atoms due to the presence of cells with few units [9], and thermodynamically stable structures [10,11]. Moreover, these MSQDs exhibit a high surface-to-volume ratio, which means that most of the atoms are located at the surface. For this reason, passivating ligands contribute a significant portion of the total number of atoms in MSQDs, and the dispersing medium can therefore dramatically affect their properties [12]. The ability to synthesize stable QDs via colloidal aqueous solutions is extremely important because it prevents the need to change the dispersion media, which thereby preserves the surface properties of the MSQDs. For medical and biotechnological applications, water-soluble QDs are needed [13,14], and appropriate functionalizations will define specific applications [15–18].

Several applications of functionalized QDs are in biomarkers and bioimaging [12,3,15–17]. In these fields, an accurate determination of the fluorescence quantum efficiency (η) is important. The present letter reports the thermo-optical properties of CdSe/CdS core–shell MSQDs in aqueous solutions by applying two techniques: the well-known thermal lens (TL) technique [19,20] and an alternative method that analyzes of the ring patterns generated in a laser beam due to thermally induced self-phase-modulation (TSPM) effects. The latter method is known as the conical diffraction (CD) technique [21,22]. Absolute nonradiative quantum efficiency or fraction thermal load (φ) and radiative quantum efficiency (η) values were determined applying TL and CD techniques. The studies were performed for CdSe/CdS core–shell MSQDs functionalized with carboxyl (R—COOH) or hydroxyl (R—OH) groups. The thermo-optical properties of the MSQDs samples, such as thermal diffusivity (D), φ and η, were determined. The results obtained for MSQDs were compared with CdSe/ZnS core–shell QDs that were non-functionalized or functionalized with carboxyl groups.

2. Theory

In TL experiments, the sample is exposed to an excitation laser beam with a GAUSSIAN intensity profile. A fraction of the absorbed energy is converted into heat, which generates a radial temperature profile $\Delta T(r, t)$. As a result of this local temperature increase, a lens-like optical element is created in the heated region. The

* Corresponding author. Fax: +55 34 32394106.
E-mail address: vivianepilla@infis.ufu.br (V. Pilla).

0009-2614/$ - see front matter © 2013 Elsevier B.V. All rights reserved.
http://dx.doi.org/10.1016/j.cplett.2013.07.007

presence of such a thermal lens can be detected by its effect on the propagation of a probing beam passing through the sample in the far-field. The temporal evolution of the on-axis probe beam intensity $I(t)$ can be calculated using integral theory in the cw excitation regime in the form [19]

$$I(t) = I(0)\left[1 - \frac{\theta}{2}\tan^{-1}\left(\frac{2\,\mathrm{mV}}{\left[(1+2m)^2+V^2\right]\tau_c/2t + 1 + 2m + V^2}\right)\right]^2 \quad (1)$$

where $m = (w_p/w_e)^2$, w_p and w_e are, respectively, the probe and excitation beam radii at the sample; $V = z_1/z_0$ where z_1 is the distance between the sample and probe beam waist and z_0 is the probe beam's Rayleigh range; and $I(0)$ is the on-axis intensity when t, or θ, is zero. $\tau_c = w_e^2/4D$ is the characteristic heat diffusion time where $D = k/\rho C$ is the thermal diffusivity (cm^2/s), k is the thermal conductivity (W/cm K), ρ is the density (g/cm^3) and C is the specific heat (J/gK). In the dual beam (excitation and probe beams) setup with a mode-mismatched configuration, the transient signal amplitude, θ, is approximately the phase difference between the probe beam at $r = 0$ and $r = \sqrt{2}\,w_e$ induced by the pump beam and is given by [18,23]

$$\theta = -\varphi\left(\frac{P_{e,abs}}{k\lambda_p}\frac{dn}{dT}\right). \quad (2)$$

In this case, $P_{e,abs} = P_e\alpha L_{eff}$, where P_e (W) is the excitation laser power, $\alpha(cm^{-1})$ is the optical absorption coefficient at the excitation wavelength (λ_e), $L_{eff} = (1-e^{-\alpha L})/\alpha$ is the effective length, L(cm) is the sample thickness, and dn/dT is the refractive index temperature coefficient. The fraction of the absorbed energy converted into heat (or the absolute nonradiative quantum efficiency) is given by [20]

$$\varphi = 1 - \eta\frac{\lambda_e}{\langle\lambda_{em}\rangle} \quad (3)$$

where λ_e is the excitation wavelength and $\langle\lambda_{em}\rangle$ is the average emission wavelength.

An analysis of the ring patterns generated in a laser beam due to thermally induced self-phase-modulation (TSPM) effects (known as the conical diffraction (CD) technique) was applied as a simple alternative method [21,22]. SPM effects can be understood from the ability of the excitation beam to induce spatial variations of the refractive index, which leads to a phase shift that depends on the transverse distance from the beam axis. This transverse self-phase modulation [21,22,24,25] is also implicated in the emergence of rings in the pattern of transmitted light when the phase change due to the nonlinearity $\Delta\phi_{NL} >> 2\pi$. The number of rings $N = \Delta\phi_{NL}/2\pi$ [25,26] in the case where the nonlinearity is a thermally induced phase change ($\Delta\phi_{TH}$), i.e. $\Delta\phi_{NL} = \Delta\phi_{TH}$, can be determined as a function of P_e by using the expression [27,28]

$$N = \frac{\varphi\alpha L_{eff}}{2\pi k\lambda_p}\frac{dn}{dT}P_e. \quad (4)$$

The interference among rays with the same wavevector that constitute the laser beam comes out parallel with different phases after traversing the nonlinear medium. The interference will be constructive or destructive in the plane of the observation if $\Delta\phi_{NL}(r_1) - \Delta\phi_{NL}(r_2) = p\pi$, where p is an even or odd integer, this is the origin of the diffraction rings [24,25].

3. Experimental

3.1. Quantum dot synthesis

Sample of CdSe/CdS core–shell MSQDs functionalized with hydroxyl (–OH) groups (QD_1, Table 1) were grown in aqueous solutions at ambient temperature. The precursors were 2 mmol of cadmium perchlorate hexahydrate ($Cd(ClO_4)_2{\cdot}6H_2O$ – 99.999%) and 4 mmol of 1-thioglycerol (>97%). Samples of CdSe/CdS core–shell MSQDs functionalized with carboxyl (–COOH) group were grown in aqueous solutions at ambient temperature. The precursors used in preparing sample QD_2 (Table 1) were 2 mmol of cadmium perchlorate hexahydrate ($Cd(ClO_4)_2{\cdot}6H_2O$ – 99.999%) and 4 mmol of mercaptoacetic acid (>98%). For sample QD_3 (Table 1), 3 mmol of cadmium perchlorate hexahydrate ($Cd(ClO_4)_2{\cdot}6H_2O$ – 99.999%) and 4 mmol of mercaptoacetic acid (>98%) were used. All reagents were purchased from Sigma-Aldrich. For CdSe/CdS MSQDs samples, the concentration was 3.7 nmol/mL, and the formation of CdSe/CdS core–shell MSQDs was based on a synthesis process [7]. In addition, solutions of non-functionalized CdSe/ZnS core–shell QDs suspended in aqueous solution (QD_4) and CdSe/ZnS core–shell QDs functionalized with carboxyl groups (QD_5) were obtained from Evident Technology at concentrations of 10 and 12 nmol/mL, respectively.

Table 1
Nomenclature for core–shell QDs samples studied in aqueous solutions.

Sample	QDs	Functionalization group	Size (nm)	$\langle\lambda_{em}\rangle$ (nm)
QD_1	CdSe/CdS	Hydroxyl	1.9	(580 ± 10)
QD_2	CdSe/CdS	Carboxyl	2.0	(584 ± 6)
QD_3	CdSe/ CdS	Carboxyl	2.3	(601 ± 9)
QD_4	CdSe/ZnS	Non-functionalized [18]	4.0	(608 ± 3)
QD_5	CdSe/ZnS	Carboxyl [18]	2.5 [18]	516 [18]

3.2. Spectroscopic characterization

The infrared (IR) spectra of the samples were recorded at room temperature on a Fourier transform infrared (FTIR) spectrophotometer (IR Prestige-21, Shimadzu) in the transmission module with a resolution of $4\,cm^{-1}$. Atomic force microscopy (AFM) images of the nanocrystalline samples were recorded at room temperature with a scanning probe microscope (SPM-9600, Shimadzu). Fluorescence spectra were recorded with a Cary Eclipse spectrophotometer (Varian) using a cuvette with 10 mm optical length.

3.3. Thermal-optical characterization

The thermo-optic properties of QDs in aqueous solutions were investigated by TL and CD techniques. TL transient measurements were performed using the mode-mismatched dual-beam (excitation and probe) configuration. A He–Ne laser ($\lambda_p = 632.8$ nm) was used as the probe beam and an Ar^+ laser ($\lambda_e = 457$ nm) was used as the excitation beam. The absorption of the relatively intense excitation beam generates the TL heat profile and the induced phase shift, which is proportional to θ. From the other side, the weak probe beam counter-propagates nearly collinearly with the excitation beam and is used to measure θ. Applying the CD technique, typical ring patterns in the far-field were observed when the sample was positioned at the focus of the Ar^+ laser beam ($\lambda_e = 457$ nm). Details of the TL and CD experimental setup can be found elsewhere [21–23].

4. Results and discussion

The sizes and size dispersions of CdSe/CdS MSQDs were determined by examining three-dimensional AFM images and their corresponding histograms [29,30]. The average sizes of the CdSe/CdS MSQDs obtained by AFM measurements (Figure 1) are presented in Table 1. Figure 2 shows the FTIR spectra for QD_1,

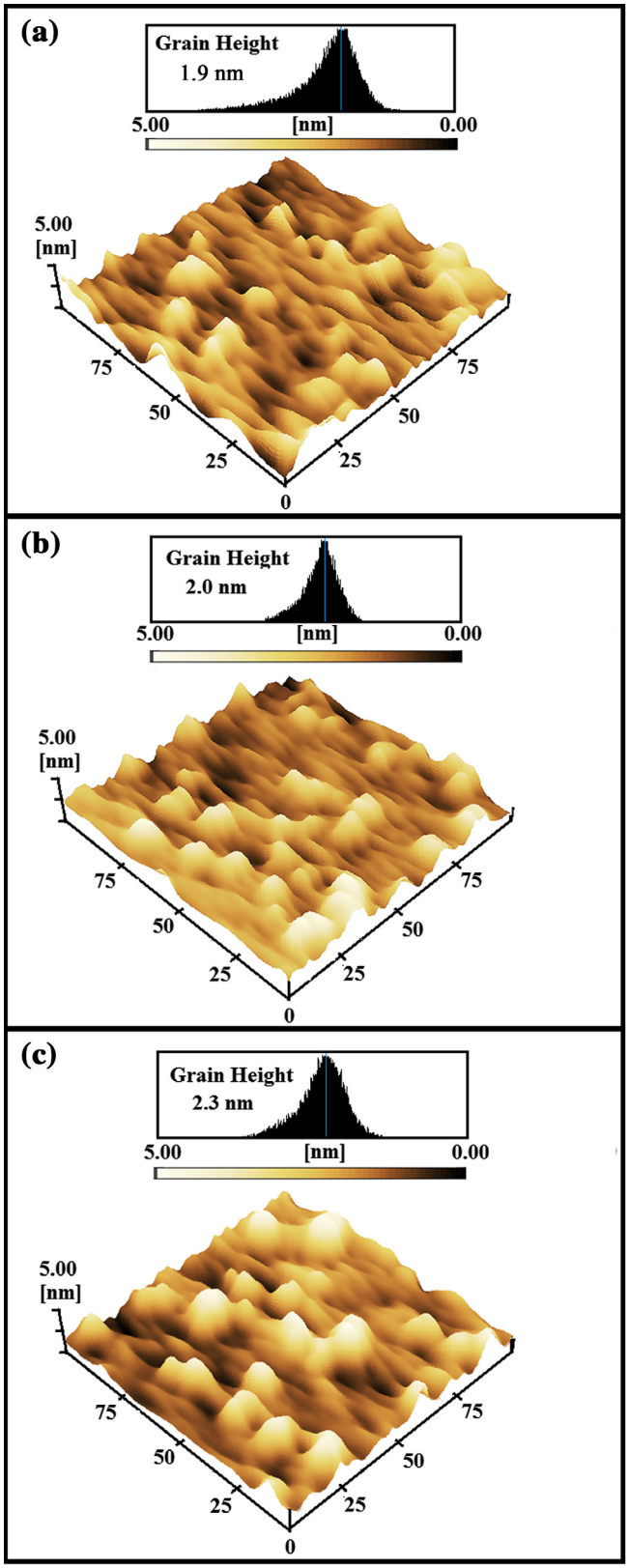

Figure 1. Room temperature AFM images and height distributions of the CdSe/CdS MSQDs samples: (a) QD_1, (b) QD_2 and (c) QD_3 (Table 1).

QD_2 and QD_3 samples (Table 1), which compare CdSe/CdS MSQDs to bulk CdS inserted in KBr pellet. The FTIR spectrum of CdS bulk presents the bandwidth with peak at 3440 cm^{-1}, which is associated with water absorption due to KBr is a hygroscopic material.

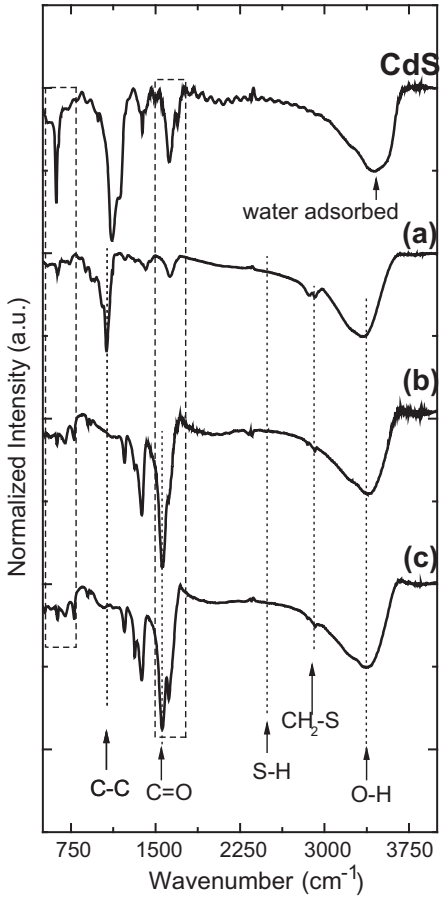

Figure 2. Room temperature FTIR spectra of CdSe/CdS MSQDs samples: (a) QD_1, (b) QD_2, (c) QD_3 and CdS bulk.

For QD_1, QD_2 and QD_3 samples a broadband in the region at 3000–3700 cm^{-1} is also presented in the FTIR spectra, but the peak shifts to ~3380 cm^{-1} due to overlapping the band of water absorbed and the characteristic OH functional group that remains intact on the surface of QDs [31]. The peaks at 867 and 2600 cm^{-1} correspond, respectively, to the bending and stretching modes of S–H bonding [32], and the peak at 2850 cm^{-1} represents CH_2–S bonding [33,34]. The spectra of the QD_2 and QD_3 samples showed peaks at 1555, 1390 and 1713–1602 cm^{-1}, which are associated with antisymmetric $\nu C{=}O$, asymmetric νCOO^- and symmetric νCOO^- vibrations, respectively [35]. These peaks confirmed that the QD_2 and QD_3 samples are functionalized with carboxylic acid groups. Spectra from the MSQDs showed that the peak at 2600 cm^{-1} representing stretching modes of S–H bonding disappears. This result confirms that a covalent bond formed between the S (of thiol) and the Cd^{+2} ions on the CdSe MSQDs surface, and these molecules act as a shell of CdS. Furthermore, based on the spectrum of bulk CdS, the spectra of all samples showed bands at approximately 619 and 1622 cm^{-1} (marked by squares) that reinforce the concept that a CdS shell has formed around the CdSe MSQDs.

Figure 3 shows typical TL transient signals for the CdSe/CdS core–shell MSQDs suspended in aqueous solutions functionalized with hydroxyl (QD_1) groups (Table 1). The behavior of the curve in Figure 3 indicates that dn/dT is negative, i.e., the created TL effect creates a defocusing of the probe beam in the far-field. By fitting the experimental data of Figure 3 by Eq. (1), θ and τ_c were obtained. Using the expression $D = w_e^2/4\tau_c$ and the measured value of w_e, the thermal diffusivity was determined for the QDs, and the D values are presented in Table 2. The average values of D obtained for the core–shell quantum dots are in good agreement with the

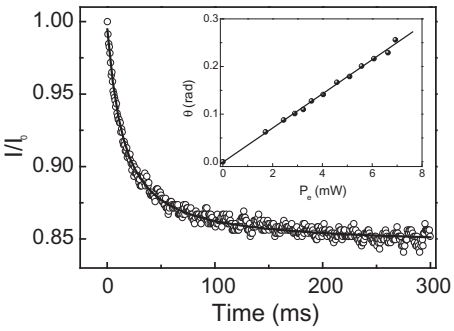

Figure 3. TL transient signal for CdSe/CdS MSQDs (QD_1) suspended in aqueous solution (λ_e = 457 nm and P_e = 4.58 mW, Table 1). The values obtained from the curve fitting were $\theta = (0.1669 \pm 0.0008)$ rad and $\tau_c = (3.58 \pm 0.05)$ ms.

Table 2
D, φ and η results obtained for QDs solutions by applying TL and CD techniques.

Sample	D (10^{-3} cm^2/s)	φ^*	η^*
QD_1	(1.50 ± 0.04)	(0.60 ± 0.08)	(0.51 ± 0.07)
QD_2	(1.5 ± 0.1)	(0.62 ± 0.05)	(0.49 ± 0.04)
QD_3	(1.5 ± 0.1)	(0.67 ± 0.06)	(0.43 ± 0.04)
QD_4	(1.54 ± 0.09)	(0.58 ± 0.09)**	(0.56 ± 0.09)**
QD_5	(1.41 ± 0.06) [18]	(0.44 ± 0.05) [18]	(0.56 ± 0.06) [18]

* Average value applying TL and CD techniques.
** Average for samples with several concentration (α = 1–4 cm^{-1}).

published values for water solvents: $D = (1.42 \pm 0.02) \times 10^{-3}$ cm^2/s [36–38]. The QDs do not significantly influence the parameters of thermal diffusivity at the concentrations analyzed in this letter. From θ, the normalized thermal parameters of the MSQDs, $\Theta = \theta/P_{e,abs}$, was determined. Using Eq. (2) and plugging the values of k and dn/dT for water [36,38], a value of φ = 0.56 was determined by TL results for QD_1 (Table 1).

Figure 4 presents the ring numbers as a function of excitation power for the QDs in aqueous solutions. By applying Eq. (4) and using the slope results for linear fitting, the values of φ (dn/dT) were determined. A standard sample of ink in water whose thermal properties are well-known was used to test the calibration of our optical system. Using the dn/dT for water [36,38] the values of φ were determined. For CdSe/CdS MSQDs functionalized with carboxyl groups (QD_2, Table 1), the φ value obtained using the CD technique was 0.64. In addition, φ = 0.60 was determined for QD_2 from the TL results. The average values for absolute nonradiative quantum efficiency obtained by applying the TL and CD techniques are presented in Table 2.

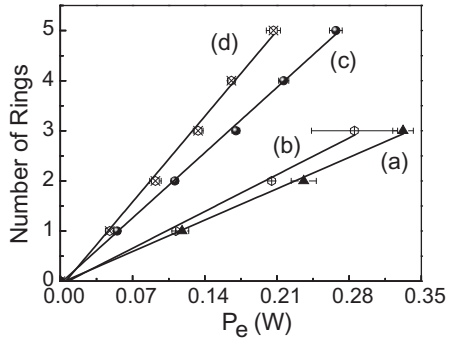

Figure 4. Number of rings (N) as a function of excitation power (P_e) for QDs suspended in aqueous solutions (λ_e = 457 nm, Table 1): (a) QD_1, (b) QD_2, (c) QD_4 and (d) ink in water (λ_e = 488 nm). The linear trend was obtained by fitting the equation $N = A^* P_e$ where the obtained A values are: (a) (9.0 ± 0.3) W^{-1}, (b) (10.6 ± 0.6) W^{-1}, (c) (18.6 ± 0.4) W^{-1} and (d) (24.4 ± 0.7) W^{-1}.

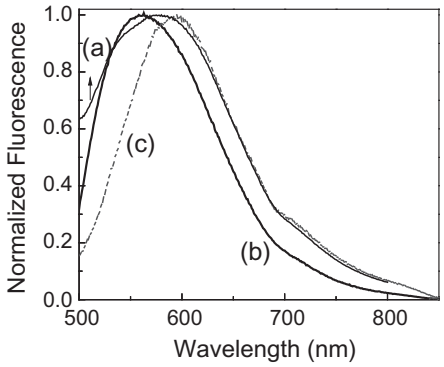

Figure 5. Normalized fluorescence spectra for (a) QD_1, (b) QD_2 and (c) QD_3 samples (Table 1, λ_e = 457 nm and 10-mm quartz cuvette).

Emission spectra for QDs suspended in aqueous solutions were measured (Figure 5), and the values obtained for $\langle\lambda_{em}\rangle$ are presented at Table 1. The values of emission bands for nanocrystals are dependent upon the concentration and the matrix in which the QDs are embedded [39]. For example, CdSe/ZnS core–shell particles suspended in solvents of chloroform and toluene have $\langle\lambda_{em}\rangle$ values of 584 and 596 nm, respectively [39]. Using φ and $\langle\lambda_{em}\rangle$ results (Tables 1 and 2), the average values of η were determined using Eq. (3), and the values are presented in Table 2 for QDs samples. In addition, radiative quantum efficiency values are presented for CdSe/ZnS particles that were non-functionalized and functionalized with carboxyl groups in aqueous solutions (Table 2). High quantum efficiencies were obtained for CdSe/CdS MSQDs functionalized with hydroxyl or carboxyl groups that were synthesized by applying the route used in this letter [7], the values were compared with the results obtained for others commercial core–shell QDs. As a comparison, quantum yield values were reported as 0.4–0.6 for CdSe QDs (sizes between 2.8 and 5.0 nm), 0.55 for CdSe/ZnSe/ZnS QDs [40] and up to 0.70 for CdTe/CdS MSQDs in aqueous colloidal solution [41]. In addition, new routes for core–shell MSQDs syntheses are in development to improve the radiative quantum efficiency of these materials.

5. Conclusions

Absolute nonradiative quantum efficiency (φ) values of functionalized CdSe/CdS core–shell MSQDs suspended in aqueous solutions were obtained using the thermal lens (TL) technique. The measurements were performed for two different functional groups: hydroxyl and carboxyl. Values of φ were obtained by measuring conical diffraction (CD) effects as a simple alternative method, and the results correlate with the TL results. High η values were obtained for the CdSe/CdS MSQDs of 1.9–2.3 nm in size in aqueous solution.

Acknowledgments

The authors are thankful to FAPEMIG, CNPq, PROPP-UFU, FAPESP and NANOBIOTEC BRAZIL for the financial support of this letter. We are also grateful for the use of the FTIR spectrophotometer (IR Prestige-21, Shimadzu) as supported by Shimadzu Brazil. The scanning probe microscope at the Institute of Physics (INFIS), Federal University of Uberlandia (UFU), was supported by the grant 'Pró-Equipamentos' from the Brazilian Agency CAPES. The Cary Eclipse spectrophotometer (Varian) was supported by NANOBIOTEC BRAZIL.

References

[1] N. Sounderya, Y. Zhang, Recent Pat. Biomed. Eng. 1 (2008) 34.
[2] M. Bruchez Jr., M. Moronne, P. Gin, S. Weiss, A.P. Alivisatos, Science 281 (5385) (1998) 2013.
[3] J. Qian, Y. Wang, X. Gao, Q. Zhan, Z. Xu, S. He, J. Nanosci. Nanotechnol. 10 (3) (2010) 1668.
[4] M.F. Frasco, N. Chaniotakis, Sensors 9 (9) (2009) 7266.
[5] A. Datta, S.K. Panda, S. Chaudhuri, J. Phys. Chem. C 111 (46) (2007) 17260.
[6] X. Chen, A.C.S. Samia, Y. Lou, C. Burda, J. Am. Chem. Soc. 127 (12) (2005) 4372.
[7] A.C.A. Silva, E.S. Freitas Neto, S.W. da Silva, P.C. Morais, N.O. Dantas, J. Phys. Chem. C 117 (4) (2013) 1904.
[8] P. Dagtepe, V. Chikan, J. Jasinski, V.J. Leppert, J. Phys. Chem. C 111 (41) (2007) 14977.
[9] V.N. Soloviev, A. Eichhofer, D. Fenske, U. Banin, J. Am. Chem. Soc. 122 (11) (2000) 2673.
[10] R. Jose, N.U. Zhanpeisov, H. Fukumura, Y. Baba, M. Ishikawa, J. Am. Chem. Soc. 128 (2) (2006) 629.
[11] K.A. Nguyen, P.N. Day, R. Pachter, J. Phys. Chem. C 114 (39) (2010) 16197.
[12] J.R. McBride, A.D. Dukes, M.A. Schreuder, S.J. Rosenthal, Chem. Phys. Lett. 498 (1–3) (2010) 1.
[13] W.W. Yu, E. Chang, R. Drezek, V.L. Colvin, Biochem. Biophys. Res. Commun. 348 (3) (2006) 781.
[14] Z.Y. Wu et al., J. Lumin. 129 (10) (2009) 1125.
[15] O.V. Salata, J. Nanobiotechnol. 2 (2004) 3, http://dx.doi.org/10.1186/1477-3155-2-3.
[16] J. Drbohlavova, V. Adam, R. Kizek, J. Hubalek, Int. J. Mol. Sci. 10 (2) (2009) 656.
[17] R. Bakalova, Z. Zhelev, D. Kokuryo, L. Spasov, I. Aoki, T. Saga, Int. J. Nanomed. 6 (2011) 1719.
[18] V. Pilla, E. Munin, J. Nanopart. Res. 14 (10) (2012) 1147, http://dx.doi.org/10.1007/s11051-012-1147-3.
[19] J. Shen, R.D. Lowe, R.D. Snook, Chem. Phys. 165 (2–3) (1992) 385.
[20] S.M. Lima, J.A. Sampaio, T. Catunda, A.C. Bento, L.C.M. Miranda, M.L. Baesso, J. Non-Cryst. Solids 273 (2000) 215.
[21] V. Pilla, E. Munin, M.R.R. Gesualdi, J. Opt. A: Pure Appl. Opt. 11 (10) (2009) 105201, http://dx.doi.org/10.1088/1464-4258/11/10/105201.
[22] A.N. Iwazaki, V. Pilla, V.M. Dias, E. Munin, A.A. Andrade, Appl. Spectrosc. 65 (12) (2011) 1393.
[23] R.A. Cruz, V. Pilla, T. Catunda, J. Appl. Phys. 107 (8) (2010) 083504, http://dx.doi.org/10.1063/1.3343517.
[24] F.W. Dabby, T.K. Gustafson, J.R. Whinnery, Y. Kohanzadeh, P.L. Kelley, Appl. Phys. Lett. 16 (9) (1970) 362.
[25] S.D. Durbin, S.M. Arakelian, Y.R. Shen, Opt. Lett. 6 (9) (1981) 411.
[26] H. Ono, I. Saito, Jpn. J. Appl. Phys. 38 (10) (1999) 5971.
[27] A.A. Andrade, T. Catunda, R. Lebullenger, A.C. Hernandes, M.L. Baesso, Electron. Lett. 34 (1) (1998) 117.
[28] T. Catunda, M.L. Baesso, Y. Messaddeq, M.A. Aegerter, J. Non-Cryst. Solids 213–214 (1997) 225.
[29] Q.K. Ong, I. Sokolov, J. Colloid Interface Sci. 310 (2) (2007) 385.
[30] A. Rao et al., J. Phys: Conf. Ser. 61 (1) (2007) 971.
[31] M.V. Artemyev, U. Woggon, H. Jaschinski, L.I. Gurinovich, S.V. Gaponenko, J. Phys. Chem. B 104 (49) (2000) 11617.
[32] D.I. Kim, M.A. Islam, L. Avila, I.P. Herman, J. Phys. Chem. B 107 (26) (2003) 6318.
[33] G. Socrates, Infrared Characteristic Group Frequencies: Tables and Charts, 2nd ed., Wiley, Chichester, 1994. p. 162.
[34] S. Komada, T. Kobayashi, Y. Arao, K. Tsuchiya, Y. Mori, Adv. Powder Technol. 23 (6) (2012) 872.
[35] J.M. Pérez-Donoso et al., PLOS ONE 7 (1) (2012) e30741, http://dx.doi.org/10.1371/journal.pone.0030741.
[36] P. Brochard, V. Grolier-Mazza, R. Cabanel, J. Opt. Soc. Am. B 14 (2) (1997) 405.
[37] V. Pilla, L.P. Alves, J.F. de Santana, L.G. da Silva, R. Ruggiero, E. Munin, J. Appl. Phys. 112 (10) (2012) 104704, http://dx.doi.org/10.1063/1.4767470.
[38] J. Georges, T. Paris, Anal. Chim. Acta 386 (3) (1999) 287.
[39] V. Pilla, L.P. Alves, E. Munin, M.T.T. Pacheco, Opt. Commun. 280 (1) (2007) 225.
[40] C.M. Donegá, M. Bode, A. Meijerink, Phys. Rev. B 74 (8) (2006) 085320, http://dx.doi.org/10.1103/PhyResB.74.085320.
[41] Z. Deng et al., J. Am. Chem. Soc. 132 (16) (2010) 5592.